

Chapter 10

Morphological Development of *Setaria viridis* from Germination to Flowering

John G. Hodge and Andrew N. Doust

Abstract The model system *Setaria viridis* is morphologically similar to other members of the Panicoideae, including maize and sorghum, although as a wild lineage it still contains a great deal of developmental plasticity. Underlying this variation is a robust ontogenetic pattern of vegetative growth resulting in the production of semi-independent basal branches (tillers) in addition to aerial branches on the main culm and tillers. We characterize the life cycle of *S. viridis* from germination to flowering and the general patterns of vegetative growth that can be expected within this period when grown under standardized conditions. We also indicate what can be expected when these plants are grown under other conditions.

Keywords *Setaria viridis* • Green foxtail • Vegetative morphology • Tillering • Branching • Flowering

10.1 Introduction

The panicoid grasses comprise approximately 3240 species (Kellogg 2001), distributed worldwide in temperate and tropical ecosystems. Several are dominants in warm-temperate prairie ecosystems, and different species have been domesticated as cereal grains in various parts of the world, including maize in central Mexico (*Zea mays*), sorghum in sub-Saharan Africa (*Sorghum bicolor*), pearl millet in southern Africa (*Pennisetum glaucum*), and foxtail millet in northern China (*Setaria italica*). The rapid growth and biomass accumulation of some wild species has also marked them as potential biofuel sources, including switchgrass (*Panicum virgatum*) and Miscanthus (*Miscanthus x giganteus*). Despite the broad agricultural and ecological importance of these grasses, basic research has been primarily focused within the domesticated cereals, with a strong focus on maize. The sexual dimorphism of terminal staminate tassel inflorescences and axillary pistillate ear

J.G. Hodge (✉) • A.N. Doust

Department of Plant Biology, Ecology, and Evolution, Oklahoma State University,
301 Physical Science, Stillwater, OK 74078, USA
e-mail: jghodge@okstate.edu

inflorescences in maize allows for easy and elegant genetic manipulation, but further functional characterization can be laborious compared to other plant models like *Arabidopsis thaliana*, given the large size of individual plants, polyploid genome, a life cycle that can take over 2 months, and difficulty of transformation (Ishida et al. 2007). In addition, maize and other domesticated panicoid cereals have highly derived phenotypes resulting from human mediated selection (Abbo et al. 2014).

Recently, *Setaria* has been suggested as a system that incorporates both a domesticated species, foxtail millet (*Setaria italica*) and its wild progenitor, green foxtail (*S. viridis*). In green foxtail, the highly inbred accession line A10.1 is being actively developed as a model for functional and developmental research [(Brutnell et al. 2010), Chaps 10, 11, 13, 14, 17–21]. *S. viridis* A10.1 (hereafter referred to simply as *S. viridis*) has many advantages that make this system more tractable as a model than maize and other agricultural counterparts. Among them are its smaller size, often only reaching 30–40 cm in height at maturity, small genome, and rapid life cycle with heading occurring roughly 21 days after germination, followed by seed maturation of the primary inflorescence within ~40 days post-germination. Alongside the capacity for high efficiency transformation through tissue culture [Chap. 20] more rapid transformation methods of *S. viridis* using floral dip protocols may also be possible [(Martins et al. 2015), (Van Eck and Swartwood 2014), Chap. 21]. *S. viridis* also benefits from a moderately large seed set (each inflorescence often bearing more than 100 seeds), allowing for easy bulking within each generation.

In this chapter, we describe the general development of *S. viridis* from germination to flowering that can be expected when *Setaria* is grown under standardized conditions. We focus primarily on vegetative development as previous work has described inflorescence development in the genus (Doust and Kellogg 2002; Doust et al. 2005). We also highlight the developmental lability of *S. viridis*, as it, along with other wild grasses, retains the capacity to recognize and respond dynamically to environmental cues during development, and can display a wide array of growth forms at maturity.

10.2 Embryology and Germination

Embryological morphology within *S. viridis* is typical of the Poaceae with embryos first being recognizable at the globular stage, where they appear as a dense, undifferentiated mass of cells embedded at the base of the developing endosperm (Fig. 10.1a). *Setaria viridis* also shows various synapomorphies unique to panicoid grasses that become more apparent at later developmental stages [Chap. 1]. Among these are the distinction between the sheathing tissue surrounding the embryonic root meristem (the coleorhiza) and the scutellum, which forms a haustorial attachment to the endosperm, resulting in a projection known as a scutellar tail (Fig. 10.1b). This distinction is absent in pooids and results in a “scutellar cleft” that is unique to panicoid species (Fig. 10.1b). Also characteristic of panicoid grasses is the

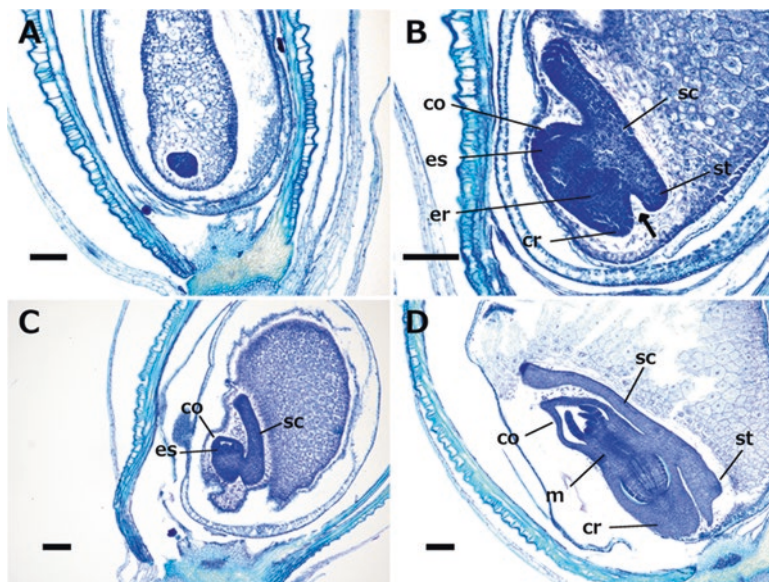


Fig. 10.1 Embryological series of *S. viridis* stained with toluidine blue. (a) Globular stage embryo appearing as a dense, undifferentiated mass of cells embedded at the base of the developing endosperm. (b) Embryo during scutellum elongation and after polarity has been established given the presence of meristematic regions for the embryonic root and shoot. Note distinctive scutellar cleft visible between coleorhiza and scutellar tail (*arrow*). (c) Embryo after juvenile leaf primordia begin initiating from the embryonic shoot meristem axis. (d) Mature embryo prior to stratification, various panicoid features are recognizable such as the distinction between coleorhiza and scutellar tail as well as a mesocotylar internode. Coleoptile (co), coleorhiza (cr), embryonic shoot meristem (es), embryonic root meristem (er), mesocotylar internode (m), scutellum (sc), scutellar tail (st), scale bars at 100 μm

elongation of the mesocotyl, producing a prominent internode between the insertion of the scutellum and coleoptile along the embryonic axis (Fig. 10.1c, d) (Kellogg 2015). In keeping with general grass development, the embryonic apical meristem remains active for a prolonged period of time, resulting in the generation of at least two leaf primordia prior to maturation of the seed (Fig. 10.1c, d) (Kellogg 2000, 2015). In keeping with the Panicoideae disarticulation pattern, seeds are abscised below the insertion of glumes so that the entire spikelet axis acts as a diaspore (Doust et al. 2014). As a result of this mechanism, the caryopsis of *S. viridis* remains encased in the sclerified sterile lower lemma and the upper palea and lemma at germination.

Germination of *S. viridis* either on petri plates or within soil media occurs in a stereotyped manner within 2–3 days after imbibition (see below). If A10.1 seeds are planted immediately after harvest, germination rates are low and highly variable. However, following seed pretreatments, *S. viridis* A10.1 usually has high germination rates (>90%) across growing conditions. Pretreatment methods include a prolonged post-harvest storage period (>1 month) between senescence of the parent plant and sowing

of the offspring, a cold shock treatment ($-80\text{ }^{\circ}\text{C}$ for 2–3 days) (Mauro-Herrera et al. 2013), or addition of liquid smoke (Jose et al. 2014; Nelson et al. 2009). Growth conditions following germination are often crucial for a normal phenotypic response given A10's sensitivity to environmental conditions. As true for most C_4 grasses, *S. viridis* prefers high light and will often exhibit either stunted growth patterns or variable morphological patterns when grown under very low light levels ($<200\text{ }\mu\text{mol m}^{-2}\text{ s}^{-1}$).

As with other panicoids such as maize and sorghum, germination follows a stereotypical pattern in which the coleoptile and mesocotyl escape through the apex of the spikelet through the aperture created by the tips of the spikelet bracts. By contrast, early radicle development is more involved, given the presence of several sclerified bracts in *S. viridis*. In cases of successful germination, there is a highly predictable pattern of radicle emergence in which the coleorhiza punctures through a germination flap at the base of the upper lemma on the spikelet in order to exit and is shortly thereafter shed by the radicle (Fig. 10.2). This pattern has also been maintained in the domesticated cultivar *Setaria italica* (Keys 1949). Previous studies have indicated that *S. italica* germinates more quickly than *S. viridis*, but our own work with *S. viridis* (A10.1) and *S. italica* (B100 and Yugu1) accessions show the opposite, indicating that speed of germination is likely genotype dependent (Keys 1949). The prolonged functionality of the coleorhiza often allows it to remain discernible on the primary axis beyond germination (Fig. 10.2d), whereas, by contrast, the coleorhiza of maize does not elongate, and thus appears minute after germination (Hochholdinger et al. 2004).

Early vegetative growth and juvenile to adult phasing when grown under standard conditions (12:12 h day:night cycle, $28\text{ }^{\circ}\text{C}$ day $22\text{ }^{\circ}\text{C}$ night, humidity $\sim 30\%$, illumination $\sim 30000\text{ }\mu\text{mol m}^{-2}\text{ s}^{-1}$).

Following emergence from the soil, *S. viridis* plants sequentially produce four juvenilized leaves that lack notable intercalary meristem growth in their corresponding internodes. The exsertion of these first four leaves occurs rapidly, with the first leaf becoming fully expanded 2 days after emergence and the ligules of the second, third, and fourth leaves appearing 6, 8, and 10 days after emergence, respectively (Fig. 10.3). There is a general increase in size with each subsequent leaf, as these juvenile leaves form a transitional grade towards the mature leaves. Gross observations suggest a similarity between the juvenile phasing of leaves in *Setaria* and those of maize (Orkwiszewski and Poethig 2000; Sylvester et al. 2001). Mature leaves under high light conditions often appear to have larger leaf areas, due to increased blade width and length, a chaffy surface, and are often more rigid. Similar features are noted within mature maize leaves, where they correlate with increases in both trichome density and vascular development (Sylvester et al. 2001). The morphology of the juvenile leaves varies little when the plants are grown at varying light intensities and densities, suggesting that the underlying developmental process is largely insensitive to environmental variation. Blade morphology beyond the first four leaves shows some relationship with environmental factors, particularly light, as when adult glasshouse-grown *S. viridis* are compared to their growth room counterparts they often have wide blades and a chaffy surface whereas adult growth room leaves are only moderately differentiated from their juvenile counterparts.

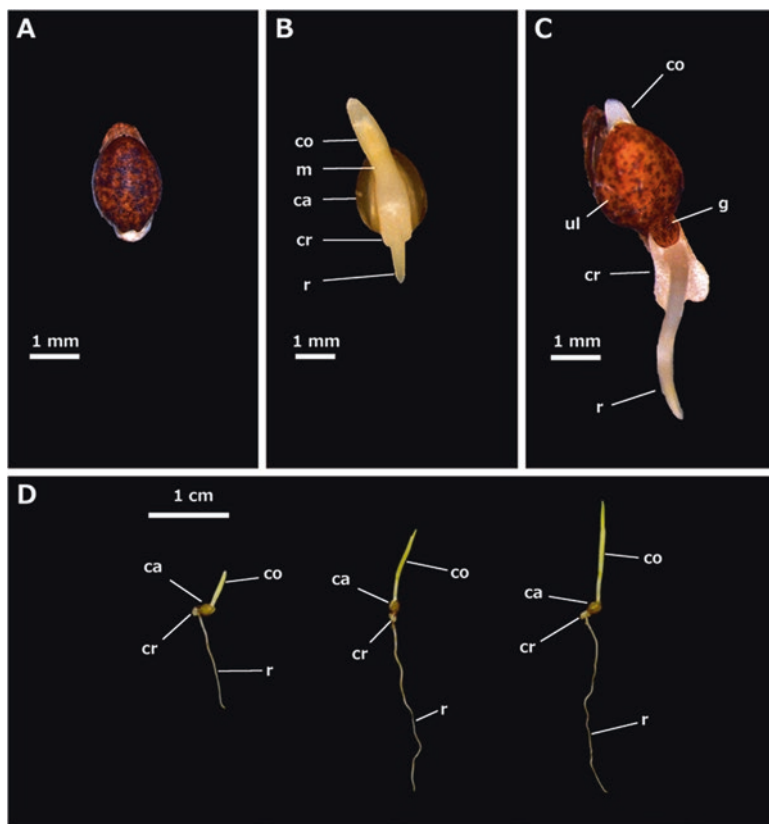


Fig. 10.2 Early germination of *S. viridis* seeds. (a) Imbibed seed prior to germination displaying mottled patterning on the surface of the upper lemma. (b) Germinating seed which has been dissected to remove the upper lemma and palea, note small rectangular coleorhiza immediately adjacent to point of attachment of the radicle to the mesocotyl. (c) Germinating seedling where the germination flap facilitating the escape of the radicle can be seen at the base of the lemma along with the coleorhiza which has continued to elongate. (d) Seedlings several hours post-germination, growth of coleorhiza arrests shortly after first leaf exserts from coleoptile and vegetative growth begins. Caryopsis (ca), coleoptile (co), coleorhiza (cr), germination flap (g), mesocotyl (m), radicle (r), upper lemma (ul)

Under standard conditions, the shoot apical meristem of *S. viridis* appears to initiate new leaves roughly every $\sim 2\text{--}3$ days (Fig. 10.4). There appears to be no delay in bud outgrowth once buds have been initiated. Linear relationships between leaf initiation and exsertion have also been shown in sorghum and maize (Clerget et al. 2008; Abendroth et al. 2011). Except for abnormally fast exsertion rates of the first two leaves (which are products of embryogenesis) maize displays a continuous rate of leaf exsertion every ~ 5.5 days, a somewhat slower rate than *S. viridis* (Abendroth et al. 2011). It is hard to disentangle if these differences in continuous growth rates are specific to distinct lineages or simply a product of domestication, as the majority of work within panicoid development has largely been focused



Fig. 10.3 Early vegetative growth of *S. viridis* under glasshouse conditions prior to axillary branch exertion. Early vegetative growth at 2 days (a), 6 days (b), 10 days (c), 14 days (d), and 18 days (f) postemergence. Numbers in (d) and (f) indicate what serial position each leaf represents in the primary axis. Axillary buds begin to elongate within 2 weeks after emerging as seen upon dissection of the 14 day (e) and 18 day (g). Numbers listed below leaf blades and their corresponding axillary buds are the serial leaf positions denoted in (d) and (f). The leaf sheaths of the first leaf of day 14 (d) and the third leaf of day 18 (f) have been pushed away from the stem by the outgrowth of the first tiller (e) and third tiller (g), respectively

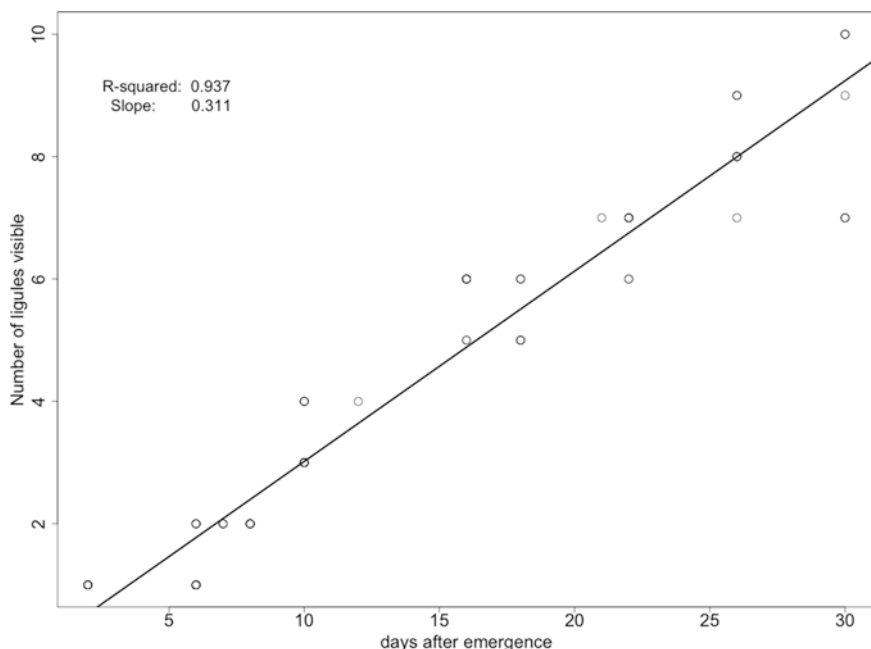


Fig. 10.4 Graph displaying periodic plastochron of *S. viridis* in which rate of leaf exertion is compared to absolute time. $m=0.311$, $R^2=0.9362$

within domesticated cereals. However, observations of *S. italica* accessions B100 and Yugu1 show rates of leaf exertion that are more comparable to those of *Z. mays*, suggesting a potential relationship between rate of organ initiation/elongation and domestication.

10.3 Axillary Branching and Root Architecture

Axillary branching occurs in two distinct phases of growth in *S. viridis*, with tillers being initiated from the basal nodes (mostly bearing juvenile leaves) and aerial branches being initiated from the nodes separated by elongated internodes along the culm and tillers. Aerial branching is often the most pronounced after the main culm has transitioned to flowering (Doust et al. 2004). The basal growth phase produces several axes (tillers) that have the potential to develop a lateral root system independent of the primary axis. Often only the first four axillary axes are near enough to the soil surface to successfully establish an independent root system and, of these, the internodes immediately associated with the first two axes are the primary sites for adventitious root initiation. Under both glasshouse conditions (14 h days with $>1000 \mu\text{mol m}^{-2} \text{s}^{-1}$ light at peak hours) and growth room conditions (12 h days and constant light $\sim 300 \mu\text{mol m}^{-2} \text{s}^{-1}$), the first discernible tillers appear in the axils of

leaves 1 and 2 at roughly 12–14 days postemergence (Fig. 10.3). Elongation of axillary buds is first recognizable by the surrounding leaf sheath being dislodged from the stalk by the rapid outgrowth of the bud (Fig. 10.3d–g). Despite being the first axes to elongate, the first and second tillers are only able to grow for a few days, producing a few juvenile leaves, before ceasing growth entirely (Fig. 10.5). The first tiller appears to always follow this pattern but the second tiller can sometimes continue growth (Fig. 10.5). This pattern becomes even more pronounced as the third and fourth tillers begin to elongate as well, often quickly overtaking their basal counterparts (Figs. 10.3 and 10.5). There are also developmental differences in the types of leaves being initiated on the first and second tillers, which primarily bear juvenilized leaves, compared to that of the third and fourth, where the first leaf is often juvenilized, and followed thereafter by mature leaves, suggesting potential differences in how these axes are developmentally canalized (Fig. 10.5). Moreover, when compared to the first two tillers, the rates of growth and leaf emergence are more uniform for the higher axes.

In accordance with studies in other grasses, the establishment of the post-embryonic root system often shows a positive correlation with tillering in *S. viridis* (Manske and Vlek 2002). Crown roots often begin to appear within a week of axillary meristem elongation, so that the crown root system occupies a comparable volume to the shoot system at flowering (Fig. 10.5). The intensity of crown root initiation varies between phytomers, often with circumscissile rings of roots initiating from the first and second internodes while only sparse root initiation is visible in the third and fourth. The exertion of these roots can have notable effects on the shoot system, with the leaf sheaths of leaves 1 and 2 often becoming severely damaged and rendered nonfunctional, and their corresponding tillers forced out of a distichous arrangement (Fig. 10.6). In some cases, the damage is more severe, with root elongation inflicting structural damage to the first and second tillers themselves. In contrast, the scarce root outgrowth from the third and fourth internodes limits damage to the surrounding sheaths and thus allows the blades of leaves 3 and 4 to remain functional until senescence. *S. viridis* shoot growth is sensitive to restrictions placed on root system growth, and plants may flower earlier if root volumes are restricted (Table 10.1).

10.4 Transition to Flowering and Inflorescence Morphology

The transition of the vegetative shoot apical meristem into the reproductive fate of an inflorescence meristem occurs when the first mature leaves are visible externally (or shortly after). Previous work in maize has suggested that a set number of phytomers is required for reproductive competency to be reached, enabling the transition of the shoot apical meristem to the inflorescence meristem (Irish and Jegla 1997). In a manner similar to many other grasses, floral transition is often first discernible in *Setaria* as the elongation of the meristematic axis into a pin-like structure, which causes it to exert beyond the shelter of the leaf primordia that cover it

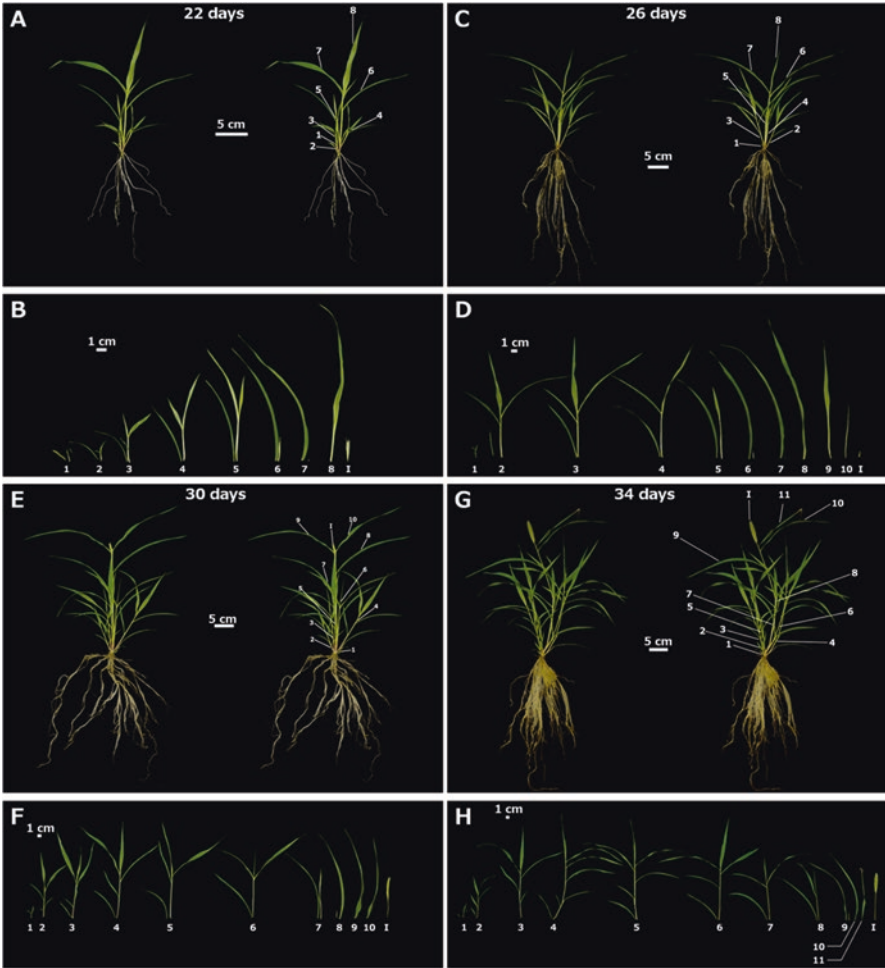


Fig. 10.5 Later vegetative growth of *S. viridis* under glasshouse conditions showing patterns of axillary branching up until flowering at 22 days (a), 26 days (c), 30 days (e), and 34 days (g) post-germination. Numbers in (a), (c), (e), and (g) indicate what serial position each leaf represents in the primary axis. Upon dissection of axillary branches, the increased growth effort in the axillary branches of the leaf 3 and 4 becomes apparent with the branches from the axils of leaves 1 and 2 showing little growth by comparison over developmental time (b), (d), (f), and (h). As the axillary branches of higher axes above the fourth leaf begin to elongate, the axillary branches usually form a developmental grade, recapitulating the order in which they were produced from the shoot apical meristem (d), (f), and (h). Numbers listed below leaf blades and their corresponding axillary branches in (b), (d), (f), and (h) are the serial leaf positions denoted in (a), (c), (e), and (g), respectively

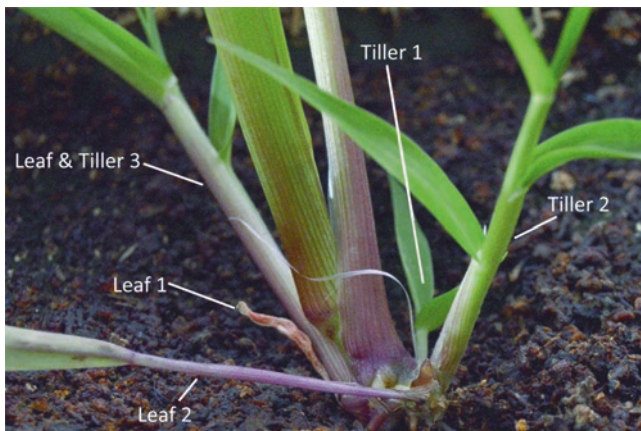


Fig. 10.6 Structural changes in first and second phytomers resulting from crown root exertion. Severe structural damage is present to sheath of the second leaf, rendering it nonfunctional. Note differences in orientation between leaves 1 and 2 compared to tillers 1 and 2, showing severity of displacement of the tillers by the secondary root system

Table 10.1 Variation in trait values for *S. viridis* in varying growth conditions, compared to standard conditions

Variable	Values	Time to flowering	Height	Branch number	Leaf number
Plant density (low to high)	Field (900 cm ² , 55 cm ²)	Same	Increased	Decreased	Not measured
Plant density (low to high)	Greenhouse (55 cm ² , 30 cm ²)	Same	Increased	Decreased	Not measured
Photoperiod (short to long)	Growth chamber (8, 12, 16 h light)	Increased	Increased	Increased	Increased
Root volume (small to large)	Greenhouse (1400 $\mu\text{mol m}^{-2} \text{s}^{-1}$: 115, 230, 345 cm ³)	Increased	Increased	Same	Same
Root volume (small to large)	Greenhouse (400 $\mu\text{mol m}^{-2} \text{s}^{-1}$: 115, 230, 345 cm ³)	Increased	Increased	Decreased	Same
Light intensity (high to low)	Greenhouse (1400, 400 $\mu\text{mol m}^{-2} \text{s}^{-1}$)	Increased	Increased	Increased	Same
Light intensity (high to low)	Growth chamber (250, 115 $\mu\text{mol m}^{-2} \text{s}^{-1}$)	Increased	Same	Decreased	Increased

These data come from unpublished growth trials (Doust, unpublished). Only trends for environmental variables that were varied within trials are noted, along with the values for those variables

during its vegetative phase (Fig. 10.7a, b). Early inflorescence development in *Setaria* bears a striking resemblance to the pistillate ears of maize at a developmentally analogous stage with primary branches being initiated acropetally (Fig. 10.7c). Unlike the paired spikelet meristems of maize resulting from these primary branches, *Setaria* undergoes a brief phase of distichous fractal-like branching along each primary branch resulting in a complex but highly repetitive morphology (Fig. 10.7d, e, h) (Doust and Kellogg 2002). The meristems produced from this process are then able to transition into either the sterile fate of bristles or fertile fate of spikelets (Fig. 10.7f). Bristles appear to be patterned from aborted spikelet meristems and are often first recognizable based on their elongated pedicels (when compared to fertile spikelets) and the circumcissile scar that forms around the base of the meristematic dome (Fig. 10.7f). Shortly after the formation of this scar, the spikelet meristem of the bristle often becomes necrotic and collapses, shedding shortly thereafter so that the apex of each bristle contains only a blunt stump, where the meristematic dome was previously attached (data not shown). By contrast, the spikelet meristems often have a short pedicel and develop as typical two-flowered panicoid spikelets, with the lower floret usually sterile (Fig. 10.7f, g). There has been some suggestion that the branching patterns of *Setaria* are an elaborated version of the paired spikelet branching pattern found within the Andropogoneae (Fig. 10.7h) (Zanotti et al. 2010). This results in the primary axis for each short branch order aborting into a sterile pedicellate axis while its recently generated axillary axis is retained as a fertile sessile spikelet (Fig. 10.7h). The combination of these growth patterns results in the characteristic arrangement of bristles surrounding the fertile spikelets of *Setaria* at maturity (Fig. 10.7i) (Doust and Kellogg 2002; Doust et al. 2005).

10.5 Environmental Sensitivity

Perhaps the most striking feature of *S. viridis* compared to other panicoid models such as maize and Sorghum is that it is a wild species and thus retains much of its phenotypic plasticity. There are various environmental stimuli which have been noted to cause phenotypic shifts, such as soil volume and depth, day length, and light quality (Doust, unpublished), as well as water stress (Fahlgren et al. 2015) (Chap. 16). Moreover, many of these developmental decisions are established early in the *Setaria* life cycle.

As an indication of the range of phenotypes that can be expected under varying growth conditions, we have compiled data from multiple unpublished trials for architectural and flowering time traits in *S. viridis* (Table 10.1). These trials vary widely in light intensity, root volume, and plant density, as well as photoperiod. Some of the differences in phenotype can be attributed to a shade avoidance response, as in the field and greenhouse density trials, where height increases, branching decreases, but flowering time stays the same. Other environmental changes affect flowering time as well, such as changing photoperiod, root volume, or light intensity. Interestingly, phenotypic responses can vary depending on the levels of an environmental variable that are

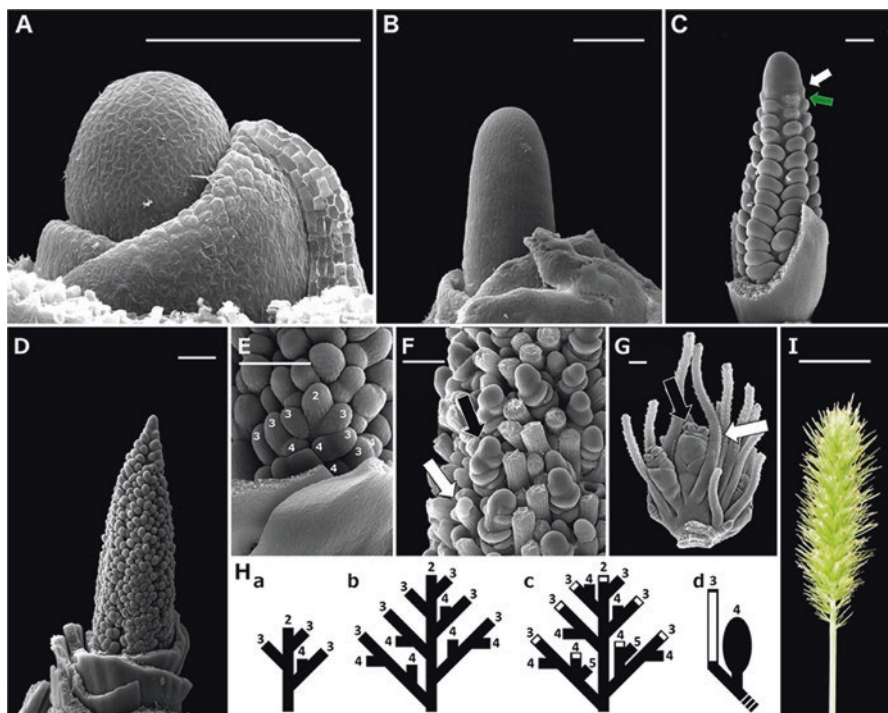


Fig. 10.7 Floral transition of the apical meristem of *S. viridis*. (A) Vegetative meristematic dome with sheathing leaf primordia removed. (B) Inflorescence meristem shortly after its floral transition causing a shift in morphology from a small dome shielded by primordia to a pin-like structure that elongates beyond the younger primordia which form a characteristic hood over the vegetative axis. (C) Primary branching phase of inflorescence development, note the small scale-like bracts (*green*) subtending each branch meristem (*white*) shortly before they elongate. (D) Formation of distichous secondary branch primordia on the primary branch axes. (E) A single axillary branch annotated so that each branch order is numbered based on its rank to the primary axis. (F) The branch meristem to spikelet meristem transition follows a typical panicoid pattern in which fertile axes (*black*) are generated that bear one or two floret meristems, or alternatively, the meristematic axis is aborted and shed so that the barren axis that eventually develops into a bristle (*white*). (G) An isolated axillary branch at a later stage of floral development showing a spikelet pair consisting of a fertile sessile spikelet (*black*) and a sterile pedicellate axis (*white*). (H) Illustration outlining branching patterns and spikelet to bristle transitions within *Setaria*. (a) Early stage of axillary branch elongation in which third-order axes are generated acropetally along the second-order axis. (b) Later developmental stage in which the patterns of the fourth branch order is recognizable and is comparable to the architecture visible in (E). (c) Transition of axes to a spikelet fate occurs shortly after (b) with terminal axes (*white*) differentiating into a sterile bristle fate whereas axillary axes are retained as fertile spikelet fates. (c) This illustration interprets the spikelet and bristle fates as analogous to a paired spikelet morphology in maize. (d) A representation of a paired spikelet to compare to (G) in which the terminal axis (*white*) has developed into a bristle, whereas the axillary axis is retained as a spikelet (*black*) and the dashed line represents the point of attachment to the lower order axis. (I) Panicle of *S. viridis* at maturity bearing both fertile spikelets and bristles. Scale bars for A–G = 100 μ m, I = 1 cm

applied. This appears to be the case for light intensity, where variation in physiologically meaningful levels of variation ($1400, 400 \mu\text{mol m}^{-2} \text{s}^{-1}$), increases flowering time, height, and branch number, but where much lower levels of light ($250, 115 \mu\text{mol m}^{-2} \text{s}^{-1}$) increase flowering time, do not affect height, and decrease branching. The sensitivity of *S. viridis* to environmental variation has the potential to be a useful tool in understanding plant–environment responses. We have made some progress in understanding the effect of photoperiod on growth and development in *Setaria* [(Orkwiszewski and Poethig 2000), Chap. 12], but much work still needs to be done to unravel the effects of carbon gain and light amount on architecture and flowering time.

10.6 Discussion

In this chapter, we have set out developmental growth patterns for *S. viridis* A10.1 from germination to flowering, with most emphasis on changes in plant architecture during growth. Like maize, *Setaria* undergoes a distinct juvenile phase in which leaves appear to be smaller at lower nodes and their corresponding internodes also reduced in size. The axillary buds of these leaves are often the most likely to develop into tillers given their proximity to the soil. Also like other cereal models, leaf initiation and exertion are highly periodic, once a meristematic axis has committed to organogenesis. There is also evidence that not all vegetative axes are equal, with the first and occasionally the second tillers arresting growth shortly after starting to elongate. We also summarize the results of several growth trials between various experiments in order to emphasize the plastic nature of this accession. It is important to be aware of the labile nature of vegetative growth in *Setaria*, as varying experimental conditions will change phenotypic outcomes, irrespective of treatments.

The other source of variation explored in this chapter is developmental, and the stages described above provide insight into growth patterns in *S. viridis* A10.1. The short life cycle means that the ontogenetic program of an individual is determined soon after germination, with developmental decisions related to branching and flowering occurring as early as the first 2 weeks following emergence. Early inflorescence development bears a superficial similarity to the ears of maize although the fractal-like branching patterns of the axillary inflorescence branches and the conversion of spikelet meristems into bristles through abortion of their meristems are both characteristic of *Setaria*. The circumcissile scars of *S. viridis* bristles resulting in spikelet meristem abortion have a resemblance to the abscission zones of spikelets although such an interpretation is at present pure speculation (Hodge and Kellogg 2016).

The underlying genetics driving plant architecture have been explored in several studies. These have implicated various architectural regulators such as *MONOCULM1*, *SEMI-DWARF1*, and *teosinte branched1* in phenotypic variation that was selected upon during the domestication of *S. italica* [(Manske and Vlek 2002), (Mauro-Herrera and Doust 2016), Chap. 12]. Much remains to be done to understand the relationship between developmental timing, environmental sensitivity, and perception, and *S. viridis* promises to be a rich source of variation and insights into these questions.

Acknowledgements We would like to thank E. A. Kellogg for permitting us to use the histological data of *S. viridis* embryology in this chapter, as well as M. S. Box who generated a scanning electron micrograph used in this chapter (Fig. 10.7g). We would also like to thank Lisa Whitworth at the Oklahoma State University Microscopy Core Facility for help with scanning electron microscopy and finally, Michael Malahy, Rene Mitchell, Josh Keegan, Cara Stephens, and Emily Harris who generated unpublished data on *Setaria* under various growth conditions.

References

- Abbo S, van-Oss RP, Gopher A, Saranga Y, Ofner I, Peleg Z. Plant domestication versus crop evolution: a conceptual framework for cereals and grain legumes. *Trends Plant Sci.* 2014;19(6):351–60.
- Abendroth L, Elmore RW, Boyer MJ, Marlay SK. *Corn growth and development*. Ames: Iowa State University; 2011.
- Brutnell TP, Wang L, Swartwood K, Goldschmidt A, Jackson D, Zhu X, Kellogg EA, Van Eck J. *Setaria viridis*: a model for C4 photosynthesis. *Plant Cell.* 2010;22:2537–44.
- Clerget B, Dingkuhn M, Goze E, Rattunde HFW, Ney B. Variability of phyllochron, plastochron and rate of increase in height in photoperiod-sensitive *Sorghum* varieties. *Ann Bot.* 2008;101:579–94.
- Doust AN, Kellogg EA. Inflorescence diversification in the panicoid “bristle grass” clade (Paniceae, Poaceae): evidence from molecular phylogenies and developmental morphology. *Am J Bot.* 2002;89(8):1203–22.
- Doust AN, Devos KM, Gadberry MD, Gale MD, Kellogg EA. Genetic control of branching in foxtail millet. *Proc Natl Acad Sci U S A.* 2004;101(24):9045–50.
- Doust AN, Devos KM, Gadberry MD, Gale MD, Kellogg EA. The genetic basis for inflorescence variation between foxtail and green millet (Poaceae). *Genetics.* 2005;169:1659–72.
- Doust AN, Mauro-Herrera M, Francis AD, Shand LC. Morphological diversity and genetic regulation of inflorescence abscission zones in grasses. *Am J Bot.* 2014;101(10):1759–69.
- Fahlgren N, Feldman M, Gehan MA, Wilson MS, Shyu C, Bryant DW, Hill ST, McEntee CJ, Warnasooriya SN, Kumar I, Ficor T, Turnipseed S, Gilbert KB, Brutnell TP, Carrington JC, Mockler TC, Baxter I. A versatile phenotyping system and analytics platform reveals diverse temporal responses to water availability in *Setaria*. *Mol Plant.* 2015;8(10):1520–35.
- Hochholdinger F, Woll K, Sauer M, Dembinsky D. Genetic dissection of root formation in maize (*Zea mays*) reveals root-type specific developmental programmes. *Ann Bot.* 2004;93:359–68.
- Hodge JG, Kellogg EA. Abscission zone development in *Setaria viridis* and its domesticated relative, *Setaria italica*. *Am J Bot.* 2016;103(6):1–8.
- Irish EE, Jegla D. Regulation of extent of vegetative development of the maize shoot meristem. *Plant J.* 1997;11(1):63–71.
- Ishida Y, Hiei Y, Komari T. Agrobacterium-mediated transformation of maize. *Nat Protoc.* 2007;2(7):1614–21.
- Jose S, Wong MK, Tang E, Dinneny JR. Methods to promote germination of dormant *Setaria viridis* seeds. *PLoS One.* 2014;9(4):e95109.
- Kellogg EA. The grasses: a case study in macroevolution. *Annu Rev Ecol Syst.* 2000;31:217–38.
- Kellogg EA. Evolutionary history of the grasses. *Plant Physiol.* 2001;125:1198–205.
- Kellogg EA. Flowering plants monocots—Poaceae. In: Kubitzki K, editor. *New York: Springer;* 2015.
- Keys CE. Observations on the seed and germination of *Setaria italica* (L.) Beauv. *Trans Kans Acad Sci.* 1949;52(4):474–7.
- Manske GGB, Vlek PLG. Root architecture—wheat as a model plant. In: Waisel Y, Eshel E, Beeckman T, Kafkafi U, editors. *Plant roots: the hidden half*. 3rd ed. New York: Marcel Dekker; 2002. p. 382.

- Martins PK, Nakayama TJ, Ribeiro AP, Dias Brito da Cunha BA, Nepomuceno AL, Harmon FG, Kobayashi AK, Molinari HBC. *Setaria viridis* floral-dip: a simple and rapid Agrobacterium-mediated transformation method. *Biotechnol Rep*. 2015;6:61–3.
- Mauro-Herrera M, Doust AN. Development and genetic control of plant architecture and biomass in the Panicoid grass, *Setaria*. *PLoS One*. 2016;11(3):e0151346.
- Mauro-Herrera M, Wang X, Barbier H, Brutnell TP, Devos KM, Doust AN. Genetic control and comparative genomic analysis of flowering time in *Setaria* (Poaceae). *G3*. 2013;3(2):283–95.
- Nelson DC, Riseborough J, Flematti GR, Stevens J, Ghisalberti EL, Dixon KW, Smith SM. Karrikins discovered in smoke trigger *Arabidopsis* seed germination by a mechanism requiring gibberellic acid synthesis and light. *Plant Physiol*. 2009;149:863–73.
- Orkiszewski JAJ, Poethig RS. Phase identity of the maize leaf is determined after leaf initiation. *Proc Natl Acad Sci U S A*. 2000;97(19):10631–6.
- Sylvester AW, Parker-Clark V, Murray GA. Leaf shape and anatomy as indicators of phase change in the grasses: comparison of maize, rice, and bluegrass. *Am J Bot*. 2001;88(12):2157–67.
- Van Eck J, Swartwood K. *Setaria viridis*. In: Wang K, editor. *Agrobacterium protocols*. New York: Springer; 2014.
- Zanotti CA, Pozner R, Morrone O. Understanding spikelet orientation in Paniceae (Poaceae). *Am J Bot*. 2010;97(5):717–29.